

# THE INTRINSIC PROPERTIES OF SDSS GALAXIES

ARIYEH H. MALLER

Department of Physics, New York City College of Technology, CUNY, 300 Jay St., Brooklyn, NY 11201

ANDREAS A. BERLIND

Department of Physics and Astronomy, Vanderbilt University, 1807 Station B, Nashville, TN 37235

AND

MICHAEL R. BLANTON, DAVID W. HOGG

Center for Cosmology and Particle Physics, Department of Physics, New York University, 4 Washington Place, New York, NY 10003

*Draft version February 2, 2008*

## ABSTRACT

The observed properties of galaxies vary with inclination; for most applications we would rather have properties that are independent of inclination, *intrinsic* properties. One way to determine inclination corrections is to consider a large sample of galaxies, study how the *observed* properties of these galaxies depend on inclination and then remove this dependence to recover the *intrinsic* properties. We perform such an analysis for galaxies selected from the Sloan Digital Sky Survey which have been matched to galaxies from the Two-Micron All Sky Survey. We determine inclination corrections for these galaxies as a function of galaxy luminosity and Sersic index. In the *g*-band these corrections reach as high as 1.2 mag and have a median value of 0.3 mag for all galaxies in our sample. We find that the corrections show little dependence on galaxy luminosity, except in the *u* band, but are strongly dependent on galaxy Sersic index.

We find that the ratio of red-to-blue galaxies changes from 1:1 to 1:2 when going from observed to intrinsic colors for galaxies in the range  $-22.75 < M_K < -17.75$ . We also discuss how survey completeness and photometric redshifts should be determined when taking into account that observed and intrinsic properties differ. Finally, we examine whether previous determinations of stellar mass give an intrinsic quantity or one that depends on galaxy inclination.

*Subject headings:* galaxies: clusters: general—galaxies: statistics—methods:statistical:surveys

## 1. INTRODUCTION

In our search to understand the formation and evolution of galaxies, some of our primary tools are measurements of the distribution of galaxy properties and relationships among these properties. From observations of these quantities at different redshifts we can deduce the nature of galactic evolution and by comparing them to the properties of dark matter halos we can constrain models of galaxy formation.

The measurement of galactic distributions includes, but is not limited to, the galaxy luminosity function (Hubble 1936), the galaxy correlation function (Peebles & Hauser 1974, the distribution of galaxies' spatial separations), the galaxy velocity function (Gonzalez et al. 2000), and the distributions of galaxy sizes (Choloniewski 1985), surface brightnesses (Freeman 1970), colors (Baum 1959; Faber 1973), metallicities (Osterbrock 1970) and star formation rates (Tinsley & Danly 1980). Relationships between galaxy properties include, the Tully-Fisher relation (Tully & Fisher 1977), the Faber-Jackson (Faber & Jackson 1976) and fundamental plane (Djorgovski & Davis 1987; Dressler et al. 1987) relations, the luminosity-size relation (Kormendy 1977), the luminosity-metallicity relation (Faber 1973; Lequeux et al. 1979) and the density-morphology relation (Dressler 1980).

However, with the notable exception of the Tully-Fisher relation these distributions and relations are tra-

ditionally measured in terms of the *observed* properties of galaxies. That is, the measurements used are K-corrected and corrected for foreground dust extinction, but no correction is attempted to compensate for the viewing angle from which the galaxies are observed. In contrast, the Tully-Fisher relation is not a relationship between a galaxy's *observed* luminosity and rotation velocity, but a relation between a galaxy luminosity and rotation velocity *corrected for inclination*. The inclination correction attempts to recover the intrinsic properties of a galaxy and not properties that are measured because of the particular angle from which the galaxy is viewed. Spiral galaxies are observed to have redder colors when their disks are more inclined, which is expected if the inclination increases the amount of dust that light traverses when emitted from the galaxy.

Clearly, we would prefer to measure all galactic distributions and relationships in terms of intrinsic galaxy properties instead of observed ones. The comparison of theory to observations is complicated and often done incorrectly because of confusion between observed and intrinsic galaxy properties. Early semi-analytic models were unable to match both the galaxy luminosity function and the Tully-Fisher relation in part because they failed to take into account that the first is observed luminosity while the second is intrinsic luminosity (Somerville & Primack 1999). Also, when comparing galaxies at different redshifts we would like to be able to distinguish between evolution in their stellar populations

and changes in their dust properties.

Furthermore, inclination effects are of great help in understanding the nature of dust in galaxies. Theoretical modeling of attenuation in galaxies is complicated because it not only depends on the properties of dust, which seem to vary between galaxies, but also on how the dust is distributed and mixed with stars. By determining the intrinsic properties of galaxies we also learn how those properties change as a function of galaxy inclination and therefore some properties of the dust distribution.

To determine intrinsic properties we need to know how a galaxy's properties change as a function of its inclination. This is different then removing the effects of dust and dust is still present for a face-on galaxy. There are a number of approaches for addressing this issue each of which has its own merits and disadvantages. One approach is to solve for an inclination correction that minimizes the scatter in the Tully-Fisher relation (e.g., Verheijen 2001), which assumes that the scatter in this relation should be as small as possible. Another method is to fit stellar population models to the SED of a galaxy and then assume that any discrepancies are caused by dust (e.g., Kauffmann et al. 2003). A third is to observe background objects behind a foreground galaxy to get a direct measure of the extinction through the galaxy (e.g., Berlind et al. 1997; Holwerda et al. 2005), but this is difficult to do for more than a handful of cases. Finally, one can simulate the radiative transfer through a galaxy (e.g., Rocha et al. 2007), assuming one knows the distribution and scattering properties of the dust.

The approach we explore here is somewhat simpler in that it assumes no knowledge of stellar population or dust properties. Instead, the main assumption is that a galaxy's properties should be independent of inclination. Thus any statistical correlation between a galaxy property and inclination can be attributed to dust and the inclination correction is whatever makes the observed correlation go away. This procedure has been applied a number of times (Giovanelli et al. 1994, 1995; Tully et al. 1998; Masters et al. 2003; Shao et al. 2007). In this paper we greatly expand upon this method by applying it to 10,340 galaxies taken from the Sloan Digital Sky Survey (SDSS, York et al. 2000) with accompanying infrared magnitudes from the Two-Micron All Sky Survey (2MASS, Skrutskie et al. 2006). It is important to have galaxies with near infrared photometry because the effects of attenuation are minimized in these wavebands (Bell & de Jong 2001). In a subsequent paper we will extend the analysis performed here to the full SDSS galaxy catalog.

We describe the method for determining inclination corrections in §2. In §3 we describe the sample we will use and discuss some of the properties of galaxies in this sample. In §4 we determine inclination corrections using our sample and compare our results to other determinations in §5. In §6 we discuss how consideration of intrinsic properties can change our conclusions about the distribution of galaxy properties focusing on the color-magnitude diagram. We also comment on the effect on survey completeness, stellar masses and photometric redshifts. §7 contains our conclusions and some discussion of future directions.

## 2. THE METHOD

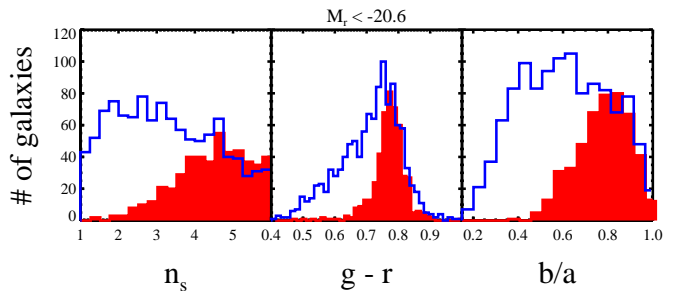


FIG. 1.— Histograms of visually classified elliptical (shaded) and disk (line) galaxies are shown in Seric index,  $n_s$ ,  $g - r$  color and axis ratio,  $b/a$ . In each case the distribution of elliptical and disk galaxies are very different. Often Seric index or color is used to divide elliptical and disk galaxies, but as is clear from the figure this still leaves many disks galaxies on the wrong side of the divide. Axis ratio can be used as a strong discriminator of galaxy type and, when combined with Seric index, gives a sample that includes 70% of all disk galaxies.

The method of determining extinction corrections statistically is based on looking for correlations between a galaxy property and galaxy inclination. Under the assumption that the intrinsic properties of galaxies do not depend on inclination, one can infer the effect of attenuation by plotting how an observed galaxy property changes with inclination. This is shown in Figure 5 for the case of galaxy color, the property we will focus on in this paper. The extinction correction then is whatever is needed to remove the observed correlation between the chosen property and galaxy inclination. Note that this procedure only measures attenuation relative to face-on galaxies, it can not say anything about the total attenuation that occurs in a galaxy.<sup>1</sup>

This method has been applied to late type galaxies where the property observed to vary with inclination is magnitude in an isophotal radius, galaxy color, or the galaxy luminosity function (Giovanelli et al. 1994, 1995; Tully et al. 1998; Masters et al. 2003; Shao et al. 2007). In order to describe these various studies within one framework we turn to a more mathematical description of the procedure.

Galaxy surveys measure a number of galaxy properties; fluxes, redshift, surface brightness, half light radius, axis ratio, position angle, etc. Fluxes are usually converted into luminosities, a quantity that doesn't depend on the galaxy's distance (it has translational invariance) using the galaxy's redshift and a K-correction. These constitute a set of observed galaxy data,  $G^o = \{M_\lambda^o, \mu^o, r_{50}^o, b/a, pa, \text{etc}\}$ . However, we would like to know the intrinsic properties of the galaxy,  $G^i$ , those properties that are invariant to rotation and translation. We assume that the two are related by a transformation,

<sup>1</sup> It is also possible that an observed correlation between a galaxy property and inclination is the result of the data reduction. Nonetheless, in this case we would still like to correct this bias. The interpretation that the correlation is caused by dust therefore does require study by analyzing the data pipeline and comparing to expectations from dust modeling. For simplicity, in this paper we will assume that dust is the dominate source of any observed correlations.

$T$ , such that

$$G^o = T(\theta, G^i)G^i \quad (1)$$

where  $T$  depends on the inclination angle of the galaxy,  $\theta$ , and possibly on other galaxy properties. If intrinsic galaxy properties do not depend on inclination then we can determine the intrinsic galaxy properties by solving for the inverse transformation  $T^{-1}$  as the operation that satisfies,

$$\left. \frac{\partial(T^{-1}G^o)}{\partial\theta} \right|_{G^i} = 0 \quad (2)$$

Note that this derivative is with respect to intrinsic galaxy properties. In practice this reduces to assuming a functional form for  $T^{-1}$  and then optimizing the parameters in that function to come as close as possible to equation 2.

One's choice about the functional form of  $T^{-1}$  therefore ends up having a strong effect on the conclusions reached. Often it is assumed that the attenuation in a given waveband,  $A_\lambda$ , is of the form

$$A_\lambda = -\gamma_\lambda \log(\cos \theta) \quad (3)$$

(Giovanelli et al. 1994, and others), where  $\gamma_\lambda$  represents the combination of dust properties, the distribution of dust and the distribution of stars that determines the attenuation at a given inclination. However, there is evidence that the dependence on inclination may be better fit by  $\log^2(\cos \theta)$  (Masters et al. 2003; Rocha et al. 2007). The parameter gamma was taken to be a constant for a given wavelength in early work (Giovanelli et al. 1994), but subsequently has been considered as a function of luminosity (Giovanelli et al. 1995; Tully et al. 1998; Masters et al. 2003; Shao et al. 2007). However, without a full understanding of the nature and distribution of dust in galaxies we can hardly know what galaxy properties  $\gamma_\lambda$  should depend on. We must rely on the data and explore what functional forms and dependencies fit best.

### 3. THE DATA

Our galaxy sample has been taken from the NYU-VAGC (Blanton et al. 2003b). We use galaxies from SDSS-DR2 that have near infrared magnitudes from 2MASS (for a discussion of the nature and completeness of these galaxies see McIntosh et al. 2006). Each galaxy has been fit in the  $r$ -band with a Sersic profile using elliptical isophotes giving us a Sersic index,  $n_s$ , a half light radius  $r_{50}$  and an axis-ratio  $b/a$ . We also have  $u, g, r, i$  and  $z$  total magnitudes from SDSS and  $J, H$  and  $K_s$  total magnitudes from 2MASS. In order to insure that our inclination measurements are accurate we restrict our sample to galaxies with a seeing-deconvolved half light radius of three or more pixels. We also restrict ourselves to fits that are within the bounds of the allowed parameter space and not at one of the limits. Thus we only include galaxies with Sersic index and inclination in the range  $0.5 < n_s < 6.0$  and  $0.15 < b/a < 1.0$ . Finally we restrict our sample to  $-17.75 \geq M_K \leq -22.75$  and  $r_{50} \leq 15\text{kpc}$ , the range where we have enough galaxies to make statistical statements about our sample. With these cuts we are left with 10,340 galaxies. Furthermore, 1,634 of these galaxies with  $M_r < -20.6$  have been visually classified by one of us (MRB). Because of the  $r$

TABLE 1  
FIT PARAMETERS TO MEAN COLORS FOR FACE-ON GALAXIES.

mean color	$v_0$	$v_K$	$v_n$	sigma	$s_0$	$s_K$	$s_n$
$\nu_{(u-K)}$	1.67	-0.27	0.26	$\sigma_{(u-K)}$	0.18	0.00	0.28
$\nu_{(g-K)}$	0.71	-0.23	0.10	$\sigma_{(g-K)}$	0.25	0.07	0.08
$\nu_{(r-K)}$	0.30	-0.20	0.02	$\sigma_{(r-K)}$	0.28	0.06	0.04
$\nu_{(i-K)}$	0.06	-0.18	0.01	$\sigma_{(i-K)}$	0.28	0.06	0.02
$\nu_{(z-K)}$	-0.02	-0.17	-0.05	$\sigma_{(z-K)}$	0.28	0.04	0.01
$\nu_{(J-K)}$	-0.01	-0.01	0.01	$\sigma_{(J-K)}$	0.12	0.04	0.01
$\nu_{(H-K)}$	-0.16	-0.02	0.00	$\sigma_{(H-K)}$	0.13	0.06	0.01

NOTE. — This table lists the values of the parameters used to fit the mean distribution of face-on galaxy colors according to equation 6 and the standard deviation about that mean according to equation 7.

selection of SDSS and K selection of 2MASS this is not a flux limited sample and thus we can not discuss the space densities of these galaxies. Therefore we will not discuss space volume at all in this paper, but will defer such discussion to a following paper that expands on our treatment here to the full SDSS galaxy catalog.

#### 3.1. Disk Galaxies

As described in §2 the method is based on identifying observed properties that depend on inclination and then removing this dependency. However, inclination is not a directly observable galaxy property. Instead, what one measures is axis ratio. Previous studies have attempted to convert axis ratio to inclination assuming a thickness for a galaxy's disk. Before one can even do this though, one has to first identify which galaxies are disk galaxies. Usually this is done by cutting the sample by concentration, Sersic index or color. Fig 1 shows histograms of the 1634 visually classified galaxies with  $M_r < -20.6$  in Sersic index,  $g-r$  color and axis ratio separately for disk (solid line) and elliptical (shaded region) galaxies. We include S0 galaxies as disk galaxies because they have a disk and therefore their measured axis ratio should be more related to the disks inclination than to the ellipticity of the spheroid component. It is clear that almost pure disk samples can be gotten by restricting one's sample to  $n_s < 3.0$  or  $g-r < 0.7$ ; however, in both these cases close to half of the disk galaxies are not included in the sample. Combining these two requirements leaves to a very mild improvement in sample completeness of only  $\sim 5\%$ . This is surprising since such cuts are often used in the literature to separate early and late type galaxy populations. It is worth noting that when such a cut is employed roughly half of the galaxies designated as early type in our sample are in fact disk galaxies.

Another property that shows a strong difference between disk and elliptical galaxies is axis ratio. Elliptical galaxies almost never have small axis ratios and galaxies with  $b/a \leq 0.55$  are 90% disk galaxies in our sample. This is understandable as disks are intrinsically thin and thus can have very small axis ratios when seen in projection, but ellipticals are close to spheroids whose intrinsic axis ratio  $q_z$ , is rarely less than 0.5 and will be larger than this when seen in projection. Thus axis ratio can be used to determine if a red concentrated galaxy is truly an elliptical galaxy or not. Since red concentrated galaxies are almost always assumed to be early-type in the literature one may be skeptical of our claim that many

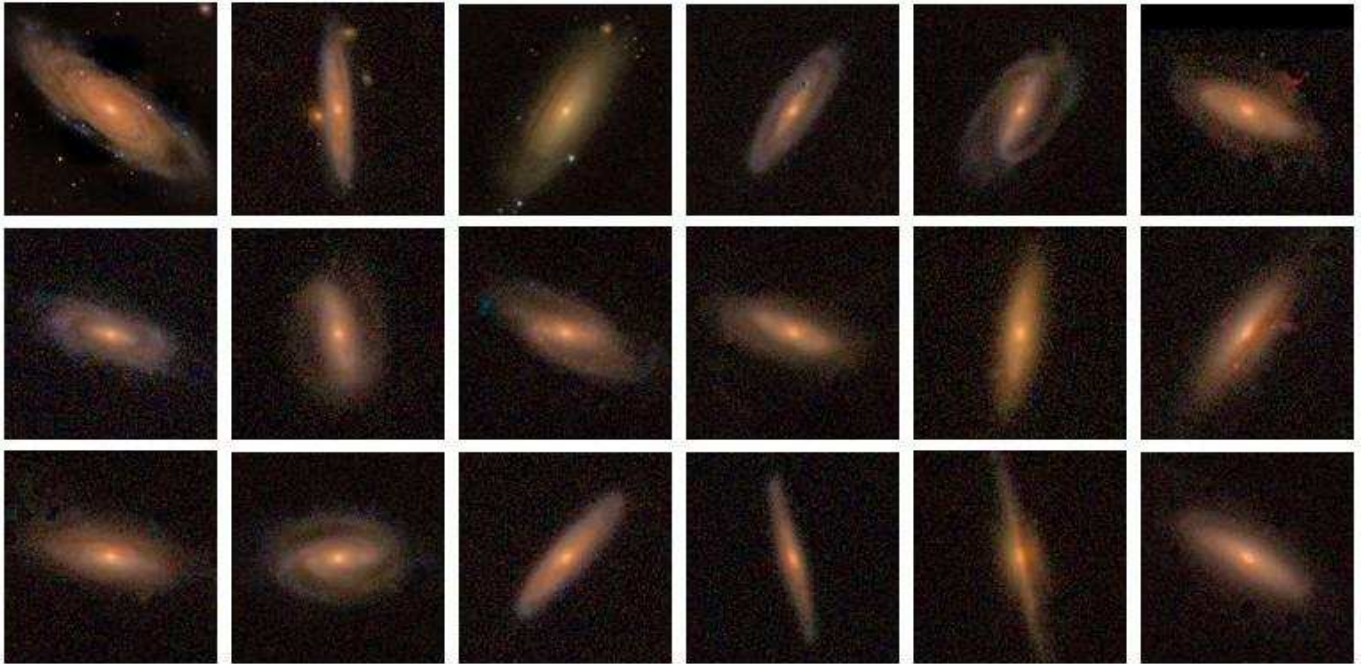


FIG. 2.— Images of red ( $g - r > 0.75$ ) and concentrated ( $n_s > 4.0$ ) and inclined ( $b/a < 0.5$ ) galaxies from our sample. Clearly these red, concentrated galaxies are disk galaxies. Besides the cuts stated the only selection in these images is that the galaxy has a large angular size so that it makes a nice image. Axis ratio is an important diagnostic of galaxy type.

of these galaxies are disk galaxies. Thus we show an example of eighteen such galaxies in Figure 2. These galaxies are selected to have  $n_s > 4.0$  and  $g - r > 0.75$  and  $b/a < 0.5$ . These are the eighteen largest galaxies (in order to make nice postage stamps) that meet the above criteria. Clearly, highly-inclined, red, concentrated galaxies are not elliptical galaxies. This is something that should be taken into account when one is trying to identify elliptical galaxies.

If we select all galaxies with  $n_s \leq 3.0$  or  $b/a \leq 0.55$  this gives a sample that is 94% disk galaxies and includes 70% of all disk galaxies. The disk galaxies missing from our sample are concentrated face-on disks. These galaxies will have the smallest inclination corrections and therefore are of the least concern for our application. However, we need these galaxies to determine if the properties of concentrated disk galaxies are changing with inclination. We discuss how we deal with this issue in §4.

### 3.2. Inclination from axis ratio

As mentioned above, the derivative in equation 2 is with respect to inclination, but inclination is not a directly measurable quantity. Previous studies have dealt with this by assuming that all disks have some average thickness and then turning the measured axis ratio into an inclination by

$$b/a = \sqrt{q_z^2 + (1 - q_z^2) \cos^2(\theta)}, \quad (4)$$

where  $q_z$  is the ratio between vertical and radial scale heights. This equation should hold if the three-dimensional light distribution is well fit by concentric ellipsoids and the disk is optically thin. However, if one examines Figure 3, which shows the distribution of observed axis ratios for galaxies with  $n_s \leq 3.0$ , binned by Sersic index, one sees that only the lowest  $n_s$  galaxies come close to having the distribution expected for randomly inclined disks with  $q_z = 0.15$ . All bins show a

deficit of face-on galaxies, which is easily understood as all sources of asymmetry in the galaxy will push one away from perfectly circular isophotes. However, for galaxies with  $n_s > 1.2$  the existence of a bulge prevents these galaxies from having very low axis ratios. We do see that galaxies with  $n_s > 1.2$  show essentially the same distribution of  $b/a$ , implying that the measured  $b/a$  is mostly correlated with galaxy inclination. Because of these measurement issues we do not believe there is a reliable way to infer a galaxy's inclination from its axis ratio. It is possible that bulge-disk decomposition fits may yield better results for the disk inclination and thus reduce this source of uncertainty. For this paper we will simply work directly with axis ratio and reform equation 2 to be that a galaxy's intrinsic properties shouldn't depend on observed axis ratio.

### 4. DEPENDENCE OF OBSERVED PROPERTIES ON AXIS RATIO

We now turn to studying the dependence of observed galaxy properties on axis ratio. We will start with galaxy color, which is the property that we have found to have the strongest dependence on axis ratio. One complication when applying the method described in §2 to the property of color is that since color is a difference between two galaxy properties the correction found will not include any correction needed to the longer wavelength magnitude. As the  $K$ -band is the longest wavelength we have access to we will consider  $\lambda - K$  colors to minimize this effect. Thus what is recovered in our case will be

$$A_\lambda = A_{\lambda, tot} - A_K - A_{\lambda, \theta=0} \quad (5)$$

where  $A_{\lambda, tot}$  is the total attenuation in a given waveband,  $A_K$  is any attenuation in the  $K$ -band and  $A_{\lambda, \theta=0}$  is any attenuation in the face-on configuration. This is why it is important to have infrared magnitudes for our sample, as we expect  $A_K$  to be relatively small (Bell & de Jong



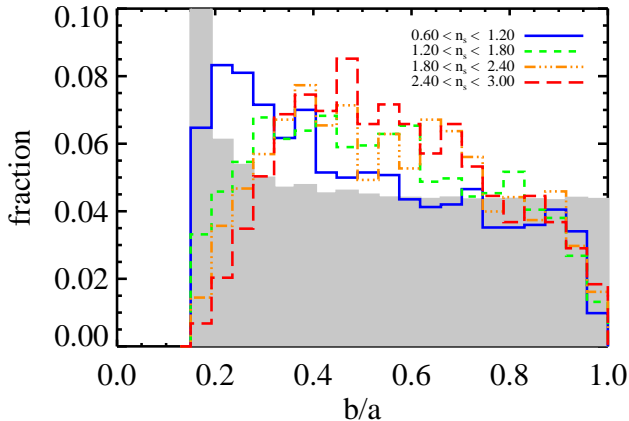


FIG. 3.— The distribution of axis ratios, for galaxies in our sample in bins of Sérsic index. The shaded region shows the theoretical expectation for the axis ratio of a randomly inclined flattened spheroid with intrinsic axis ratio,  $q_z = 0.15$ . For all bins there is a deficiency of nearly circular galaxies compared to theory as is expected since any asymmetry in the light profile will move the isophotes away from circular. Galaxies with  $n_s > 1.2$  have nearly the same distribution of axis ratios. Only the least concentrated galaxies have an axis ratio distribution similar to that of randomly oriented disks with finite thickness. Even a small bulge reduces the ellipticity of a galaxy’s isophotes. Nonetheless, it is evident that axis ratio is mostly a measure of galaxy inclination.

2001). In this section we will only show figures for  $g - K$  colors, but our analysis is done for all six  $\lambda - K$  colors we can produce. To see the analogous figures for other wavebands please look at the supplemental online material or visit the website [www.galaxystats.com/intrinsic/](http://www.galaxystats.com/intrinsic/).

In order to determine how a given galaxy’s color depends on its inclination we need to know what that galaxy’s color should be if we could see it face-on. Figure 4 shows the distribution of  $g - K$  colors of face-on disk galaxies ( $b/a > 0.85$ ) as a function of  $K$ -band luminosity and Sérsic index. The first two panels show all face-on galaxies with  $n_s \leq 3.0$  while the third panel shows the face-on galaxies with  $n_s > 3.0$  that have been visually classified as disk galaxies by one of us (MRB). We only include the visually classified galaxies because we do not want to include elliptical galaxies, even though this means we are sampling a different luminosity range than the first two panels. We see that color depends on both Sérsic index and luminosity which are not independent of one another. The relationship looks close to linear for absolute magnitude and linear in Sérsic index to a value of  $n_s = 4.0$  at which point it appears to flatten out. Based on this we will assume that the dependence on  $M_K$  and  $n_s$  are separable and fit the mean galaxy color by a function of the form

$$\nu_{(\lambda-K)} = v_0 + v_K(M_K + 20) + v_n n_{\text{eff}} \quad (6)$$

where  $\nu_{(\lambda-K)}$  is the average  $M_\lambda - M_K$  color of a face-on galaxy with absolute magnitude  $M_K$  and Sérsic index  $n_s$  and  $n_{\text{eff}} = n_s$  for  $n_s \leq 4.0$  and  $n_{\text{eff}} = 4.0$  for  $n_s > 4.0$ . The values of  $v_0$ ,  $v_K$  and  $v_n$  that best fit the data are shown in Table 1. One sees that the dependence of color on  $n_s$  is relatively weak except for  $u - K$  colors, so this truncation for  $n_s \leq 4.0$  generally has very little effect.

As can be seen in Figure 4, the dispersion about this mean also varies with  $M_K$  and  $n_s$ , so we also fit the standard deviation with the formula

$$\sigma_{(\lambda-K)} = s_0 + s_K(M_K + 20) + s_n n_{\text{eff}}. \quad (7)$$

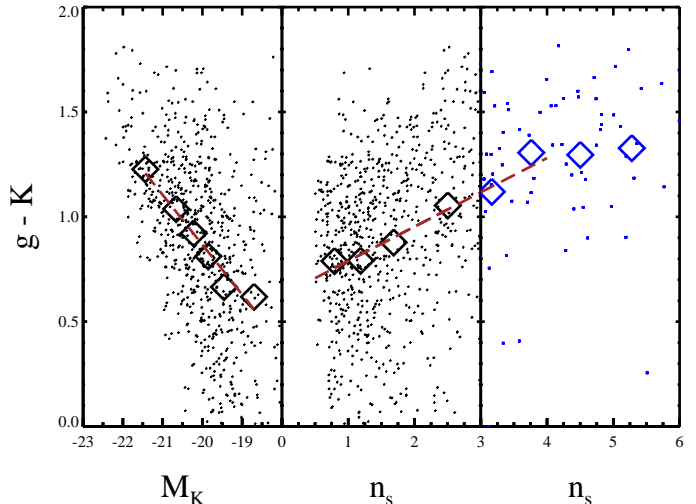


FIG. 4.— The  $g-K$  color of face-on galaxies ( $b/a > 0.85$ ) is shown versus  $M_K$  in the left panel and  $n_s$  in the right two panels. Diamonds show the mean value in a bin. For  $n_s > 3.0$  (the right panel) we only plot galaxies visually classified as disks to avoid any confusion with ellipticals. The sample in the right panel is thus different than in the first two panels. In spite of this, it is clear that galaxy color is a function of luminosity and Sérsic index. In both cases the mean relationship is close to linear, with evidence for a flattening for  $n_s > 4.0$ .

Again we use a value of  $n_{\text{eff}} = 4.0$  for  $n_s > 4.0$  galaxies just to be consistent with equation 6. Values of the fit parameters for dispersion are also given in Table 1. One can see that the dependence on  $n_s$  is weak and whether or not one flattens the relationship at  $n_s = 4.0$  will have very little effect on our results. In all cases, we find that these simple linear functions provides an adequate fit to the mean galaxy color and the standard deviation about this mean.

With a model for the mean color of a face-on galaxy, we can now investigate how galaxy colors deviate from their mean face-on value as a function of axis ratio. Figure 5 shows  $g - K$  color minus  $\nu_{(g-K)}$  versus  $\log b/a$ , for different bins of Sérsic index. In all cases, a strong relationship is seen and one that seems to be roughly linear in  $\log b/a$ . The large intrinsic scatter in galaxy color makes it difficult to judge whether a more complicated dependence on  $\log b/a$  is warranted. As a linear relationship seems adequate, we will express the attenuation in the form

$$A_\lambda = -\gamma_\lambda \log b/a. \quad (8)$$

Note that this is different than what has been done historically where the attenuation is considered to be linear in  $\log(\cos \theta)$  (equation 3). Here we are expressing the attenuation in terms of the observed axis ratio. It would be very interesting to compare this to the dependence of attenuation on observed axis ratio in radiative transfer simulations.

Examining Figure 5, we see that  $\gamma_\lambda$  (the slope of the line) varies with Sérsic index. Creating plots like Figure 5 and dividing the sample by other galaxy properties, we find that the correlation between color and axis ratio is strongest when binned by  $n_s$  or  $M_K$ . Therefore we uncover that  $\gamma_\lambda$  depends on at least these two parameters. We start with the simplest assumption, that  $\gamma_\lambda$  can be determined from a linear combination of these paramete-

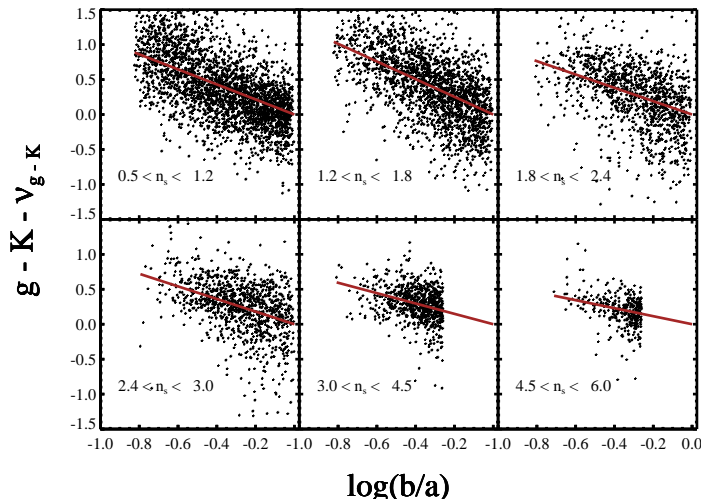


FIG. 5.— The difference between a galaxy’s  $g - K$  color and the mean value of the  $g - K$  color for a face-on galaxy with the same  $M_K$  and  $n_s$  is shown as a function of axis ratio for six different bins of  $n_s$ . We see in all cases, even for the highest  $n$  bin, there is a clear trend for more inclined galaxies to be redder. The relationship seems to be linear in  $\log b/a$  with a slope that becomes shallower with higher  $n$ .

ters:

$$\gamma_\lambda = \alpha_0 + \alpha_K(M_K + 20) + \alpha_n n_{\text{eff}}, \quad (9)$$

where the parameters  $\alpha_0$ ,  $\alpha_n$  and  $\alpha_z$  depend on wavelength. Again we will assume that dependence flattens off for  $n_s > 4.0$ . Note that previous studies have only considered a linear dependence on luminosity, not Sersic-index. Now that we have a model for the attenuation we can investigate the best fit parameters for equation 9. To do this we use a Monte Carlo Markov Chain (MCMC) to minimize the statistic,

$$\chi^2 = \sum \left[ \frac{(M_\lambda - A_\lambda - M_K) - \nu_{(\lambda-K)}}{\sigma_{(\lambda-K)}} \right]^2 \quad (10)$$

where  $A_\lambda$  is given by equations 8 and 9. The resulting best fit parameters are shown in Table 2. Figure 6 shows the effect of using these corrections to determine the intrinsic colors of galaxies in our sample. Plotted is the intrinsic  $g-K$  color versus axis ratio for our disk galaxy sample. We see that, unlike in Figure 5, there is not a discernible correlation between galaxy color and axis ratio. Thus, it seems that our simple linear functions are sufficient to describe the behavior of the attenuation. When Figure 6 is made for the other 5 wavebands, a similar lack of correlation is seen.

Table 2 also gives the mean value of  $\gamma_\lambda$ , the mean value of the attenuation and the maximum attenuation of any galaxy in our sample for each waveband. We see that in the  $g$  band the attenuation can be as large as 1.25 magnitudes, but that the mean attenuation is 0.28 magnitudes. These values decrease substantially with longer wavebands reaching a mean attenuation of only a few hundredths of a magnitude for the near infrared bands. We expect any attenuation in the  $K$ -band to be less than this and thus negligible.

As a semi-independent check of our results, we compare the distribution of  $M_g$  magnitudes and  $g - r$  colors for  $n_s \leq 3.0$  galaxies in our sample. We restrict ourselves to

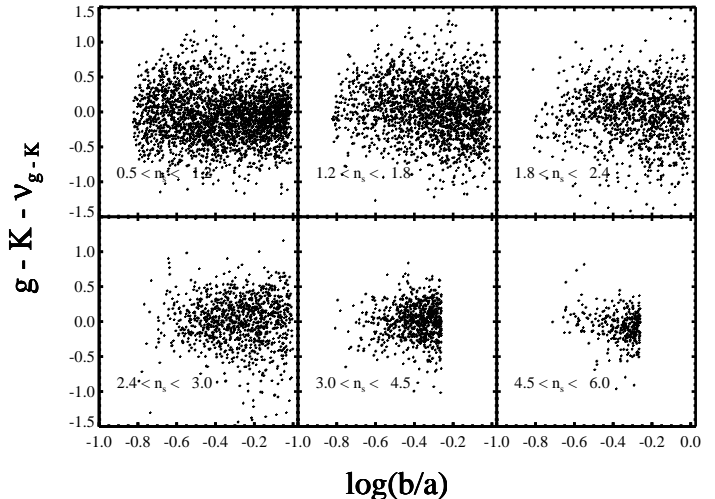


FIG. 6.— The difference between a galaxy’s intrinsic  $g - K$  color (corrected for inclination) and the mean value of the  $g - K$  color for a face-on galaxy with the same  $M_K$  and  $n_s$  is shown as a function of axis ratio for six different bins of  $n_s$ . We see that applying the inclination correction removes the dependence of color on inclination seen in Fig 5.

these low concentration galaxies so that we can compare face-on ( $b/a \geq 0.85$ ) and edge-on ( $b/a \leq 0.30$ ) disk galaxies without having contamination from ellipticals. The distributions of these quantities for face-on (shaded), uncorrected edge-on (dashed line) and corrected edge-on (solid line) galaxies is shown in Figure 7. One sees that the distributions of face-on and edge-on galaxies is significantly different. The mean  $M_g$  magnitude and  $g - r$  color of face-on galaxies are  $-19.2$  and  $0.54$ , respectively; for edge-on galaxies the values are  $-18.6$  and  $0.71$ . This significant difference is dramatically reduced when considering the corrected magnitudes of the edge-on galaxies, which have mean values of  $-19.3$  and  $0.56$ , respectively. Examination of the histograms in Figure 7 shows that while corrected  $g - K$  colors have nearly the same mean as the face-on colors, there is some difference in the shape of the distribution. This seems to be an indication that an additional parameter or possibly a cross term is needed to fully describe the correction, though this is difficult to tell since there is a small bias introduced because edge-on galaxies are included in the sample based on their observed and not their intrinsic magnitudes. Either way, these differences are relatively small and the overall success of our inclination corrections is evident.

Having determined the correction for magnitudes we now turn to another galaxy property that shows inclination dependence, galaxy size. Our measured half light radii  $r_{50}$  are only in the  $r$ -band, though it would be very informative for dust modeling to look at the radial dependence of attenuation in different wavebands. Examining the face-on sizes of galaxies in our sample we see that they depend on  $K$ -band luminosity (i.e., the Kormandy relation, Kormandy 1977), but show no dependence on sersic index. We find the mean face-on half light radii are well fit by

$$\log r_{50} = 0.5 - 0.13(M_K + 20). \quad (11)$$

The distribution around this value is roughly lognormal as seen in previous studies (de Jong & Lacey 2000; Shen et al. 2003) so we will perform our correction in  $\log r_{50}$ . Comparing edge-on to face-on galaxies we find

TABLE 2  
INCLINATION CORRECTION PARAMETERS FOR DIFFERENT WAVE  
BANDS

Band	$\alpha_0$	$\alpha_K$	$\alpha_n$	max $\gamma_\lambda$	mean $A_\lambda$	max $A_\lambda$
$A_u$	1.79	-0.43	-0.28	1.31	0.39	1.88
$A_g$	1.38	-0.19	-0.22	0.94	0.28	1.24
$A_r$	1.02	-0.09	-0.12	0.78	0.23	0.88
$A_i$	0.90	-0.05	-0.14	0.60	0.18	0.70
$A_z$	0.56	0.01	-0.01	0.53	0.15	0.46
$A_J$	0.31	-0.02	-0.07	0.17	0.05	0.24
$A_H$	0.15	0.01	-0.05	0.05	0.02	0.11

NOTE. — The table shows the parameters used to fit for  $\gamma_\lambda$  to determine the attenuation in different bands according to eqns. 8 and 9. Also shown are the mean and maximum attenuation in each waveband and the maximum value of  $\gamma_\lambda$ .

that galaxies with  $n_s \leq 2.0$  have larger half light radii when they are inclined. For galaxies with  $n_s > 2.0$  we see no effect, probably because of the prominence of bulges in these galaxies. This increase of the sizes of inclined galaxies is what one would expect if there is more dust in the inner parts of galaxies causing greater attenuation in the center. However, as noted earlier, this may also be an artifact of the data pipeline used to determine galaxy size or a combination of both dust and the data pipeline. We parametrize the effect for galaxies by the formula

$$\log r_{50}^i = \log r_{50}^o + \beta_r (\log b/a) \quad (12)$$

where  $r_{50}^i$  and  $r_{50}^o$  are the intrinsic and observed half light radii, respectively, and  $\beta_r$  is the strength of the effect in the  $r$ -band (analogous to  $\gamma_\lambda$ ). Minimizing  $\chi^2$  gives values of  $\beta_r = 0.2$ . We find that we do not need luminosity or sersic index dependence to bring the edge-on galaxies into agreement with the face-on galaxy size distribution. This can be seen in the third panel of Figure 7 which shows the face-on and the corrected edge-on galaxy size distributions to be in good agreement. It will be interesting to continue this analysis for the full SDSS galaxy catalogue as we plan to in a following paper. Having determined corrections for observed magnitudes and sizes of galaxies in our sample, we now turn to comparing our results to previous determinations of the inclination correction in the literature.

## 5. COMPARISON TO PREVIOUS WORK

In comparing our results to previous work it is important to take into account three differences in our treatment. One, our value of  $\gamma_\lambda$  is multiplied by  $\log b/a$  instead of  $\log(\cos \theta)$ . Two, we explore  $\gamma_\lambda$  dependence on both  $M_K$  and  $n_s$ , while earlier studies only considered dependence on luminosity. Finally, we include all types of galaxies in our sample instead of focusing on just late type galaxies.

Our values of  $\gamma_\lambda$  for an  $n_s = 1.0$  galaxy are shown as a function of galaxy luminosity in Figure 8. One sees that aside from in the  $u$ -band, the dependence on luminosity is fairly weak. For comparison, we show the values determined by Tully et al. (1998); Masters et al. (2003) and Shao et al. (2007). Note that Shao et al. found no evidence for luminosity dependence, so their fit assumes this and that  $\gamma_\lambda$  has a power law dependence on wavelength. Also, to compare to Tully et al., we have converted the measured dependence to  $M_K$  by subtracting

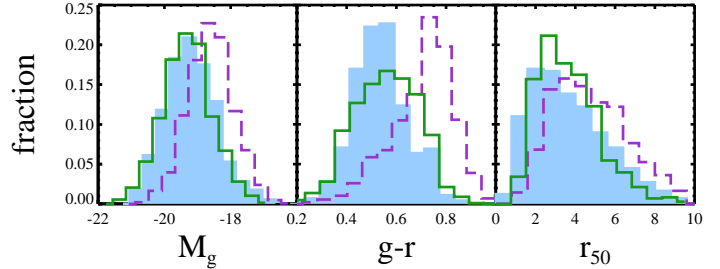


FIG. 7.— The left most panel shows the distribution of observed  $g$ -band magnitudes for face-on (shaded) and edge-on (dashed line) galaxies. Also shown is the distribution of intrinsic (corrected) magnitudes for the edge-on (solid line) galaxies. One sees that the distributions of observed magnitudes is very different, but that once an inclination correction has been applied the distributions become almost identical. The middle panel shows distributions of  $g - r$  color, with the same line-styles as the left most panel. Again the inclination corrections bring the edge-on galaxies into agreement with the face-on ones. However, the shape of the corrected color distribution differs from the face-on one, suggesting that there may be dependence on another parameter needed for the correction. The right most panel shows the distribution of observed galaxy half light radii,  $r_{50}$ , again with the same line styles indicating observed face-on, observed edge-on and intrinsic edge-on galaxies. In all three panels only galaxies with  $n_s \leq 3.0$  are used to insure a fair comparison.

the mean  $r - K$  and  $i - K$  colors of our galaxy sample. We see that the determinations of  $\gamma_\lambda$  from all studies have similar values, that is they all agree with one another at some luminosity. However, the dependence on luminosity shows a wide range of behaviors. There are many possible reasons for these differences. One is definitely the assumptions that have been made, for example the  $\gamma_I$  value from Masters et al. assumes no luminosity dependence, while the  $\gamma_J$  values is fit to a broken line. Clearly, we expect that we will get different results because we have fit to both luminosity and Sersic index. Other issues that may be important are the sample selection used in the study, the conversion from  $b/a$  to inclination done in the other studies, and which property is being correlated with inclination. Tully et al. and we both used galaxy color, while Masters et al. looked at magnitude in an isophotal radius and Shao et al. focused on the galaxy luminosity function. In particular, as we have shown in §4, not only is the total luminosity of a galaxy dependent on axis ratio, but also the half light radius is too. Since isophotal radius depends on both it may not be surprising that we arrive at different results than Masters et al. These intricacies will require further study, which would be most enlightening when combined with radiative transfer simulations.

The dependence of  $\gamma_\lambda$  on Sersic index is shown in Figure 9. In general, we find that the dependence on Sersic index is stronger than on  $K$ -band magnitude. We have fit each band independently so the unphysical situation that arises in Figure 9 can occur where  $\gamma_z$  becomes larger than  $\gamma_i$  at high Sersic index. This is of course undesirable, but our approach is to investigate what we can learn from the data instead of coming in with theoretical prejudices. One can easily find an acceptable solution to this

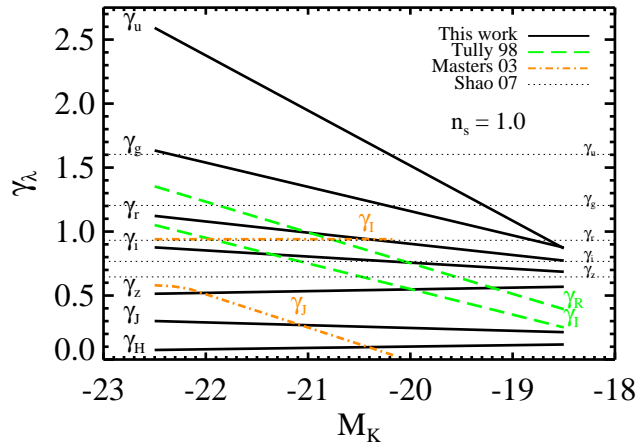


FIG. 8.— The value of  $\gamma_\lambda$  for spiral galaxies ( $n_s = 1$ ) as a function of  $M_K$  is shown in comparison to other results from Tully et al. (1998, dashed lines), Masters et al. (2003, dash-dot lines) and Shao et al. (2007, dotted lines). Note that none of the wavebands are the same (except for the  $J$ -band which are all from 2MASS) and that the methods used to determine  $\gamma_\lambda$  all differ.

by requiring that  $\gamma_\lambda$  is always smaller in longer wavelengths. That would mean that in Figure 9,  $\gamma_z$  would take on the value of  $\gamma_i$  where now  $\gamma_z > \gamma_i$ . One way to improve in this area would be to fit multiple wavelengths at the same time, under some assumptions about how the attenuation at different wavelengths is related.

Since we fit each waveband independently and since  $\gamma_\lambda$  depends on both  $M_K$  and  $n_s$ , the wavelength dependence on  $\gamma_\lambda$ , and thus the attenuation, varies with  $M_K$  and  $n_s$ . Figure 10 shows the wavelength dependence of  $\gamma_\lambda$  for fixed values of  $M_K$  and  $n_s$ . We see that generally a power law is a good fit to  $\gamma_\lambda$  in the SDSS wavebands. The index of the power law seems to increase with  $M_K$  for fixed  $n_s$ , while at fixed  $n_s$  the slope of the index of the power law remains almost unchanged and only the amplitude of  $\gamma_\lambda$  increases with decreasing  $n_s$ . The power law index ranges from  $\sim 0.5$  to  $\sim 1.5$ . These relationships should be very useful in understanding the distribution of dust in these galaxies. We see in all cases  $\gamma_\lambda$  in the near infrared bands ( $J$  and  $H$ ) falls below the power law fit. It is clear from this that the amount of attenuation in the  $K$ -band, not included in our calculations, is negligible.

We conclude from this that the corrections we find are in general agreement with previous results and that differences are probably primarily due to our including the dependence on Sersic index. We now turn to a preliminary exploration of how galaxy properties differ when considering the intrinsic instead of observed values.

## 6. INTRINSIC GALAXY PROPERTIES COMPARED TO OBSERVED ONES

In this section we turn to comparing intrinsic galaxy properties to observed ones. A complete discussion of this subject is beyond the scope of this work. And as we have mentioned earlier, we will not be discussing the space density of objects because we do not have a flux limited sample. Instead we will focus on how galaxy photometric quantities change in our sample when going from observed to intrinsic properties. The overall effect is fairly modest, as can be seen from Table 2, the average attenuation in the  $g$ -band is  $A_g = 0.28$ . This will

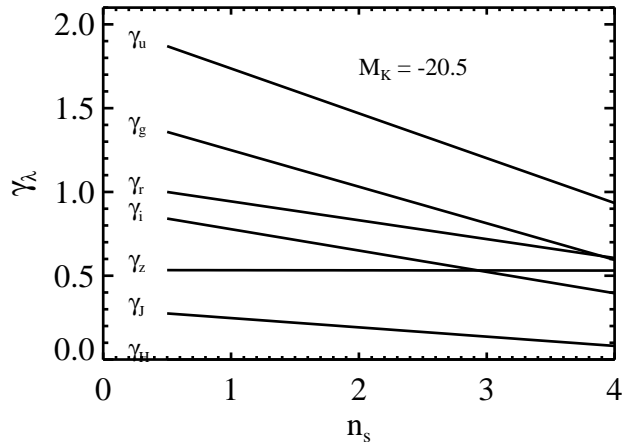


FIG. 9.— The value of  $\gamma_\lambda$  as a function of Sersic index.  $\gamma_\lambda$  shows a strong dependence on Sersic index in all bands except for the  $z$ -band.  $\gamma_z$  shows almost no dependence on  $n_s$ , which becomes unphysical when  $\gamma_z \geq \gamma_i$ . This seems to imply that our assumption that  $\gamma_\lambda$  is linear in  $n_s$  should be modified. Unfortunately, unlike in Fig. 8 we can not compare our results as other studies have not calculated  $\gamma_\lambda$  as a function of Sersic index.

have small effects on the galaxy luminosity function and correlation function, essentially a small shift in their amplitudes. However, the inclination correction is not uniform, and while many galaxies have no correction others are brightened by up to 1.25 magnitudes in the  $g$ -band. Thus the most notable effect will be in comparing the properties of spiral and elliptical galaxies. We will focus on the differences between observed and intrinsic galaxy color as seen in the color magnitude diagram, the determination of stellar masses, and the determination of photometric redshifts, all measurements that are based on galaxy color. First though, we start with discussing survey completeness.

### 6.1. survey completeness

When information is presented from a galaxy survey it is usually taken from a flux limited catalog. The SDSS spectroscopic sample is complete to an apparent magnitude of  $m_r = 17.7$ . This can be converted to an equivalent completeness in observed absolute magnitude at some distance. But this does not translate into an equivalent completeness in intrinsic magnitudes. Thus, when one looks at a flux limited catalog, there are galaxies that are intrinsically identical to galaxies in the catalog, but are excluded because of the inclination they happen to be viewed at. When discussing the distribution of galaxy properties or connecting galaxies to dark matter halos this is not desirable. In intrinsic magnitudes, the survey is only complete to the maximum attenuation brighter than the observed magnitude. So in the  $r$ -band, where the maximum attenuation is  $\sim 0.9$  magnitudes, this corresponds to  $m_r = 16.8$  a much shallower survey.

If one wants an intrinsically complete survey it is not necessary to obtain spectra for every galaxy fainter than the survey limit down to this maximum attenuation. Instead one only needs to target galaxies where

$$m_r < 17.7 + \max(\gamma_r) * \log b/a \quad (13)$$

a much smaller sample of galaxies. If one determines Sersic indices before targeting the galaxies then  $\max(\gamma_r)$



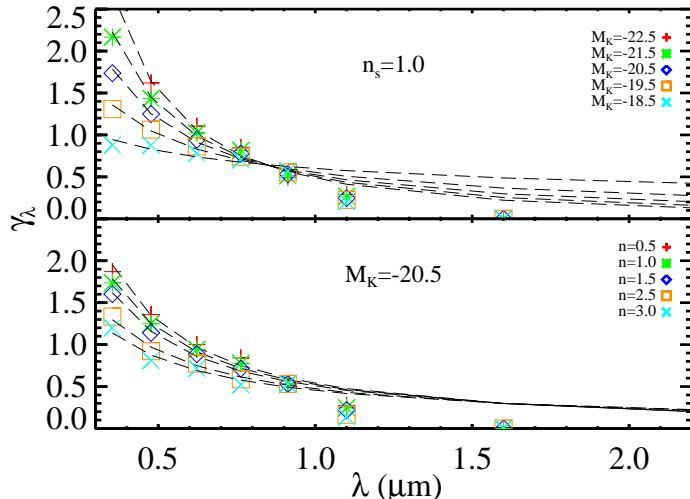


FIG. 10.— The value of  $\gamma_\lambda$  as a function of wavelength for various values of  $M_K$  at fixed  $n_s$  (top panel) and for various values of  $n_s$  at fixed  $M_K$  (bottom panel). The lines are power law fits to the 5 values for the SDSS bands. One sees that though the first 5 bands seem to be well fit by a power law the measured values of  $\gamma_J$  and  $\gamma_H$  are always well below the extrapolation of this curve.

would equal the maximum value of  $\gamma_r$  for that value of  $n_s$ . Without the Sérsic indices (or some equivalent measure) one would have to use the maximum value of  $\gamma_r$  which for our sample is 1.1. To give an example, we use the DR4 sample of SDSS, which does not have determinations of Sérsic indices, but has measured axis ratios, though different than the ones we have been using in this paper (see §3). These axis ratios are measured with exponential fits (labeled `ab_exp` in the catalog), but are reasonably close to the ones we have been using which are based on elliptical Sérsic fits. In this sample there are 92,752 galaxies with  $m_r < 16.8$ . Going 0.9 mag deeper to  $m_r < 17.7$  increases the sample by 242,103 galaxies. However, if the axis ratio of the galaxy is considered then there are only 89,855 galaxies that may be brighter than 16.8 mags after correcting for inclination. Thus taking the axis ratio into account reduces the required follow up spectra by 63%. Future surveys may want to consider axis-ratio along with apparent magnitude when determine their galaxy sample. In this way, samples limited to some intrinsic magnitude can be compiled which will greatly facilitate comparisons to theory and other observations.

### 6.2. color-magnitude relationship

One area where we see a significant difference between observed and intrinsic properties is in the color-magnitude diagram. Figure 11 shows a color-magnitude diagram for observed and intrinsic magnitudes for our sample. There is no  $1/V_{max}$  weighting as explained earlier, which would increase the difference between the two plots. Clearly, the distribution of points has changed in the two panels. In the observed color-magnitude diagram 46% of galaxies have  $g - r \geq 0.7$ ; for the intrinsic color-magnitude diagram this decreases to 32%. Therefore, in observed colors the split between red and blue is roughly 1:1, in intrinsic color this changes to 1:2. Assertions about how the galaxy population is evolving based on the number of red or blue galaxies (Faber et al. 2005; Bell et al. 2007) should probably look at changes in in-

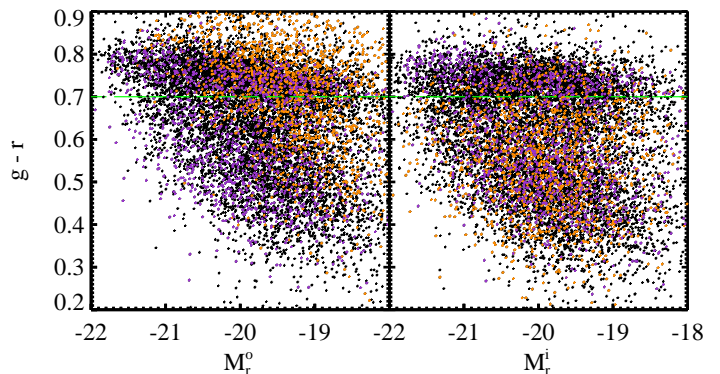


FIG. 11.— The observed color-magnitude diagram (left panel) and the intrinsic color-magnitude diagram (right panel). In the observed color magnitude diagram there are many galaxies redder than the red sequence. These galaxies are mostly removed in the intrinsic color-magnitude diagram. Face-on ( $b/a > 0.85$ ) and edge-on ( $b/a < 0.35$ ) galaxies are color coded by purple and orange, respectively. In the left panel they occupy a completely different region of the diagram, but in the right panel they have similar distributions.

trinsic instead of observed properties if they want to be sure that reddening isn't a large part of the effect they are measuring.

### 6.3. stellar masses

One intrinsic galaxy property that we have not discussed yet is stellar mass. Stellar mass is not directly observable, but there are a number of methods that try to estimate the stellar mass based on spectroscopy or photometry, (Bell et al. 2003; Blanton et al. 2003a; Kauffmann et al. 2003). Clearly, stellar mass is an intrinsic property - the mass of a galaxy shouldn't change under rotation. To check that this is the case then, one would like to see that equation 2 holds for stellar mass. Figure 12 shows histograms of the stellar mass for face-on ( $b/a \geq 0.85$ , shaded) and edge-on ( $b/a \leq 0.3$ , line) galaxies using the mass estimates of Kauffmann et al. (2003), Blanton et al. (2003a) and Bell et al. (2003). We see that in the estimates of Kauffmann et al. edge-on galaxies are slightly less massive than face-on galaxies, that for Blanton et al. edge-on galaxies are slightly more massive than face-on galaxies and that for Bell et al. there is remarkably good agreement between the two. We should note that the method of Kauffmann et al. is based on spectra which, for the low redshift sample we are considering will only probe the inner parts of a galaxy and therefore is more likely to be in error. Also, we are only testing that the determined stellar mass does not depend on inclination not that it is the correct value of the stellar mass. The point of this exercise is just to demonstrate that one should check that intrinsic quantities actually don't show dependence on inclination.

### 6.4. photometric redshifts

Finally, we turn to the issue of determining photometric redshifts (e.g., Hogg et al. 1998) for galaxies, or clusters found by identifying red-sequence galaxies (e.g Koester et al. 2007), which is a subset of photometric

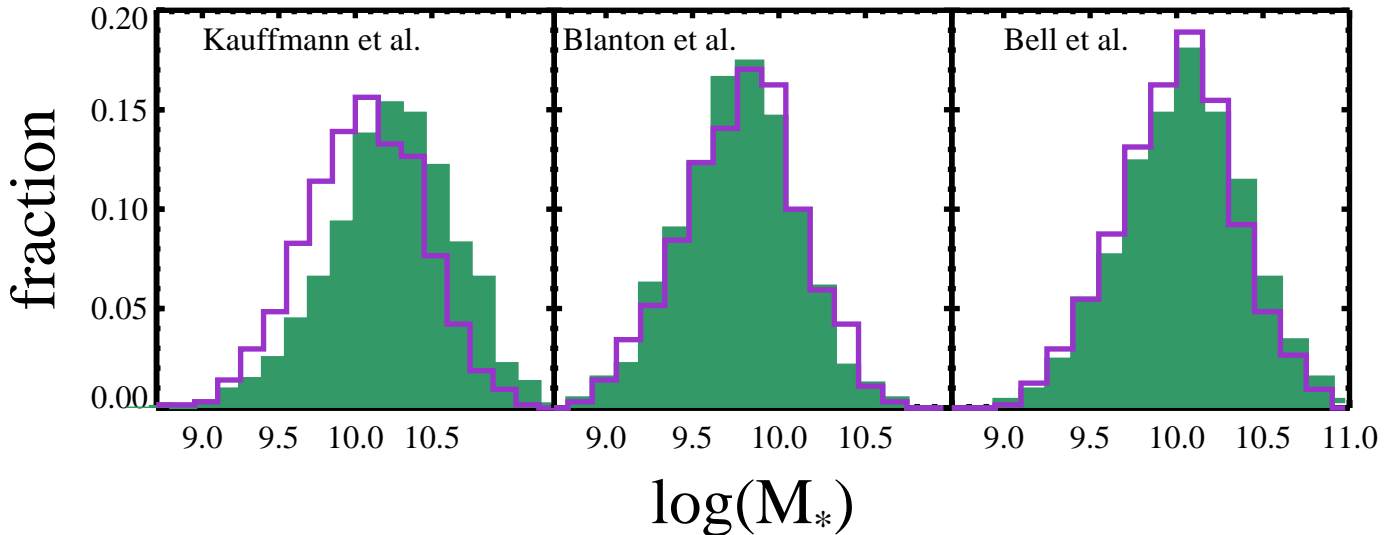


FIG. 12.— The distribution of stellar masses in our sample for face-on (shaded) and edge-on (line) galaxies with  $n_s \leq 3.0$ . The left panel shows stellar masses determined by Kauffmann et al. (2003), the middle panel by Blanton et al. (2003a) and the right panel by Bell et al. (2003). We see that in the left panel the edge-on galaxies are not corrected enough, in the middle panel they are corrected too much and for the right panel the correction is just right. Note that this only tests that there is not inclination dependence in the determination, not that the stellar masses are correct.

redshifts. In recent years algorithms to determine a galaxy’s redshift only using photometric redshifts have become very successful. These methods rely on the fact that there is a limited family of intrinsic SEDs that galaxies have so that with enough wavelength coverage it is possible to determine both the galaxy’s SED and redshift with only photometric data. However, as we have demonstrated in this paper, the observed SED of a galaxy changes with inclination. It may still be possible to disentangle the intrinsic SED, reddening and redshift with observations in enough wavebands, but in cases where an axis ratio can be measured, photometric redshifts ignore useful information. Thus we strongly recommend that in future determinations of photometric redshifts axis ratio be used to help reduce uncertainties.

## 7. CONCLUSION

This paper has focused on the intrinsic properties of galaxies, which are routinely determined for Tully-Fisher studies (e.g., Pizagno et al. 2007), but not for other statistical studies of galaxies. Intrinsic properties are invariant under changes in viewing angle, unlike observed properties which would change if we could view a galaxy from a different vantage point. Our main goal in this paper has been to clarify the difference between observed and intrinsic properties and to suggest how observed properties can be converted into intrinsic ones.

The method we use in this paper is to identify an observed galaxy property that shows a correlation with axis ratio and then apply the necessary correction to remove this correlation. We find that both color and size show

correlations with axis ratio. We are able to remove these correlations using simple linear formula that depend on  $K$ -band magnitude and Sersic index. We therefore can construct a galaxy catalog with intrinsic value for galaxy size and magnitude.

There are many distributions and relationships that should be reconsidered in terms of the intrinsic properties instead of the observed ones. We can not cover all of these in a paper of this length but we highlight a few points to suggest how things may change. We focus on the color magnitude diagram as an example. The observed color magnitude diagram shows a number of galaxies redder than the red sequence and a lack of bright blue galaxies. When we plot the intrinsic color magnitude diagram these ultra red galaxies are mostly removed and there are many more bright blue galaxies. We find that the ratio of blue to red galaxies changes from 1:1 to 2:1 for galaxies with absolute luminosities  $-23.75 \geq M_K > -17.75$ , a significant change.

In a following paper, we apply the insights we have gained here to producing inclination corrections for the full SDSS catalog. Having intrinsic properties for this flux limited catalog will then allow us to address how volume densities are effected when going from observed to intrinsic quantities.

AHM is grateful for many fruitful conversations with Martin Weinberg during the conception of this project. We would like to thank Eric Bell, James Bullock and Dan McIntosh for helpful comments on earlier

drafts of this paper. AHM was partially supported by GRTI-CT05AGR9001 and PSC-CUNY-60021-36-37 grants from CUNY. MRB was partially supported during this work by grants NASA-06-GALEX06-0030, NSF-AST-0607701, and Spitzer G03-AT-30842M.

Funding for the SDSS and SDSS-II has been provided by the Alfred P. Sloan Foundation, the Participating Institutions, the National Science Foundation, the U.S. Department of Energy, the National Aeronautics and Space Administration, the Japanese Monbukagakusho, the Max Planck Society, and the Higher Education Funding Council for England. The SDSS Web Site is <http://www.sdss.org/>.

The SDSSf is managed by the Astrophysical Research Consortium for the Participating Institutions. The Participating Institutions are the American Museum of Natural History, Astrophysical Institute Potsdam, University of Basel, University of Cambridge, Case Western Reserve University, University of Chicago, Drexel Uni-

versity, Fermilab, the Institute for Advanced Study, the Japan Participation Group, Johns Hopkins University, the Joint Institute for Nuclear Astrophysics, the Kavli Institute for Particle Astrophysics and Cosmology, the Korean Scientist Group, the Chinese Academy of Sciences (LAMOST), Los Alamos National Laboratory, the Max-Planck-Institute for Astronomy (MPIA), the Max-Planck-Institute for Astrophysics (MPA), New Mexico State University, Ohio State University, University of Pittsburgh, University of Portsmouth, Princeton University, the United States Naval Observatory, and the University of Washington.

This publication makes use of data products from the Two Micron All Sky Survey, which is a joint project of the University of Massachusetts and the Infrared Processing and Analysis Center/California Institute of Technology, funded by the National Aeronautics and Space Administration and the National Science Foundation.

## REFERENCES

- Baum, W. A. 1959, *PASP*, 71, 106  
 Bell, E. F. & de Jong, R. S. 2001, *ApJ*, 550, 212  
 Bell, E. F., McIntosh, D. H., Katz, N., & Weinberg, M. D. 2003, *ApJS*, 149, 289  
 Bell, E. F., Zheng, X. Z., Papovich, C., Borch, A., Wolf, C., & Meisenheimer, K. 2007, *ApJ*, 663, 834  
 Berlind, A. A., Quillen, A. C., Pogge, R. W., & Sellgren, K. 1997, *AJ*, 114, 107  
 Blanton, M. R., Brinkmann, J., Csabai, I., Doi, M., Eisenstein, D., Fukugita, M., Gunn, J. E., Hogg, D. W., & Schlegel, D. J. 2003a, *AJ*, 125, 2348  
 Blanton, M. R., et al. 2003b, *ApJ*, 594, 186  
 Choloniewski, J. 1985, *MNRAS*, 214, 197  
 de Jong, R. S. & Lacey, C. 2000, *ApJ*, 545, 781  
 Djorgovski, S. & Davis, M. 1987, *ApJ*, 313, 59  
 Dressler, A. 1980, *ApJ*, 236, 351  
 Dressler, A., Lynden-Bell, D., Burstein, D., Davies, R. L., Faber, S. M., Terlevich, R., & Wegner, G. 1987, *ApJ*, 313, 42  
 Faber, S. M. 1973, *ApJ*, 179, 731  
 Faber, S. M. & Jackson, R. E. 1976, *ApJ*, 204, 668  
 Faber, S. M. et al. 2005, *ArXiv Astrophysics e-prints*  
 Freeman, K. C. 1970, *ApJ*, 160, 811  
 Giovanelli, R., Haynes, M. P., Salzer, J. J., Wegner, G., da Costa, L. N., & Freudling, W. 1994, *AJ*, 107, 2036  
 —. 1995, *AJ*, 110, 1059  
 Gonzalez, A. H., Williams, K. A., Bullock, J. S., Kolatt, T. S., & Primack, J. R. 2000, *ApJ*, 528, 145  
 Hogg, D. W., et al. 1998, *AJ*, 115, 1418  
 Holwerda, B. W., González, R. A., Allen, R. J., & van der Kruit, P. C. 2005, *A&A*, 444, 101  
 Hubble, E. 1936, *ApJ*, 84, 270  
 Kauffmann, G. et al. 2003, *MNRAS*, 341, 33  
 Koester, B. P., McKay, T. A., Annis, J., Wechsler, R. H., Evrard, A. E., Rozo, E., Bleem, L., Sheldon, E. S., & Johnston, D. 2007, *ApJ*, 660, 221  
 Kormendy, J. 1977, *ApJ*, 218, 333  
 Lequeux, J., Peimbert, M., Rayo, J. F., Serrano, A., & Torres-Peimbert, S. 1979, *A&A*, 80, 155  
 Masters, K. L., Giovanelli, R., & Haynes, M. P. 2003, *AJ*, 126, 158  
 McIntosh, D. H., Bell, E. F., Weinberg, M. D., & Katz, N. 2006, *MNRAS*, 373, 1321  
 Osterbrock, D. E. 1970, *QJRAS*, 11, 199  
 Peebles, P. J. E. & Hauser, M. G. 1974, *ApJS*, 28, 19  
 Pizagno, J., Prada, F., Weinberg, D. H., Rix, H.-W., Pogge, R. W., Grebel, E. K., Harbeck, D., Blanton, M., Brinkmann, J., & Gunn, J. E. 2007, *AJ*, 134, 945  
 Rocha, M., Jonsson, P., Primack, J. R., & Cox, T. J. 2007, *ArXiv Astrophysics e-prints*  
 Shao, Z., Xiao, Q., Shen, S., Mo, H. J., Xia, X., & Deng, Z. 2007, *ApJ*, 659, 1159  
 Shen, S., Mo, H. J., White, S. D. M., Blanton, M. R., Kauffmann, G., Voges, W., Brinkmann, J., & Csabai, I. 2003, *MNRAS*, 343, 978  
 Skrutskie, M. F. et al. 2006, *AJ*, 131, 1163  
 Somerville, R. S. & Primack, J. R. 1999, *MNRAS*, 310, 1087  
 Tinsley, B. M. & Danly, L. 1980, *ApJ*, 242, 435  
 Tully, R. B. & Fisher, J. R. 1977, *A&A*, 54, 661  
 Tully, R. B., Pierce, M. J., Huang, J.-S., Saunders, W., Verheijen, M. A. W., & Witchalls, P. L. 1998, *AJ*, 115, 2264  
 Verheijen, M. A. W. 2001, *ApJ*, 563, 694  
 York, D. G. et al. 2000, *AJ*, 120, 1579